doi:10.1016/j.jmb.2006.08.010 J. Mol. Biol. (2006) 363, 648–659

JMB

Available online at www.sciencedirect.com

ScienceDirect

ELSEVIER

# Structure of the Blm10–20 S Proteasome Complex by Cryo-electron Microscopy. Insights into the Mechanism of Activation of Mature Yeast Proteasomes

**Jack Iwanczyk[1], Kianoush Sadre-Bazzaz[2], Katherine Ferrell[2] Elena Kondrashkina[3], Timothy Formosa[2], Christopher P. Hill[2] and Joaquin Ortega[1]***

[1]*Department of Biochemistry and Biomedical Sciences McMaster University 1200 Main Street West Hamilton, Ontario Canada L8N 3Z5*

[2]*Department of Biochemistry University of Utah School of Medicine, 15 North Medical Drive East, Salt Lake City UT 84112-5650, USA*

[3]*Biophysics Collaborative Access Team (BioCAT), BCPS Department, Illinois Institute of Technology, 3101 S. Dearborn Chicago, IL 60616, USA*

**Corresponding author*

The 20 S proteasome is regulated at multiple levels including association with endogenous activators. Two activators have been described for the yeast 20 S proteasome: the 19 S regulatory particle and the Blm10 protein. The sequence of Blm10 is 20% identical to the mammalian PA200 protein. Recent studies have shown that the sequences of Blm10 and PA200 each contain multiple HEAT-repeats and that each binds to the ends of mature proteasomes, suggesting a common structural and biochemical function. In order to advance structural studies, we have developed an efficient purification method that produces high yields of stoichiometric Blm10–mature yeast 20 S proteasome complexes and we constructed a three-dimensional (3D) model of the Blm10–20 S complex from cryo-electron microscopy images. This reconstruction shows that Blm10 binds in a defined orientation to both ends of the 20 S particle and contacts all the proteasome α subunits. Blm10 displays the solenoid folding predicted by the presence of multiple HEAT-like repeats and the axial gates on the α rings of the proteasome appear to be open in the complex. We also performed a genetic analysis in an effort to identify the physiological role of Blm10. These experiments, however, did not reveal a robust phenotype upon gene deletion, overexpression, or in a screen for synthetic effects. This leaves the physiological role of Blm10 unresolved, but challenges earlier findings of a role in DNA repair.



*Keywords:* Blm10; PA200; proteasome activator; cryo-electron microscopy; three-dimensional reconstruction

## Introduction

The 20 S proteasome in yeast is a cylindrical particle of 28 subunits arranged as four heptameric stacked rings.[1–3] The two rings at the ends, the α rings, comprise seven catalytically inactive subunits that are similar but distinct proteins, named α1 to α7. Similarly, the two central rings, the β rings, are formed by seven different β subunits, three of which house active sites at their N termini.[3] In order to fulfill all its different functions, the 20 S proteasome binds to a number of proteins that deliver substrates, stimulate the peptidase/protease activity and may target the proteasome complex to specific locations in the cell. These include the 19 S regulatory particle (RP),[4,5] the 11 S activator (PA28/PA26/REG)[6–9] (not present in yeast) and PA200,[10] all of which bind to the ends of the 20 S proteasome. The two ends of the

Abbreviations used: cryo-EM, cryo-electron microscopy; WT, wild-type; ORF, open reading frame; CTF, contrast transfer function; FSC, Fourier shell correlation.

E-mail address of the corresponding author: ortegaj@mcmaster.ca

cylindrically shaped 20 S proteasome can bind either the same or different regulatory particles forming homogeneous or hybrid proteasomes, respectively.[10–13]

The PA200 activator was initially found in mammals[10] and electron microscopy (EM) studies showed that it binds to the ends of the 20 S proteasome and opens the axial channel into the proteolytic cavity.[14] The PA200 sequence contains multiple HEAT-like repeats suggesting that the protein adopts a solenoid structure.[15] The sequences of PA200 and the yeast Blm10 (formerly known as Blm3[16,17]) proteins are 20% identical (41% similar) over the 1715 C-terminal residues of each protein. Conservation of this class of proteasome activators from yeast to humans suggests an important and evolutionarily conserved biological role. Like PA200, Blm10 binds to the ends of mature 20 S proteasomes and is predicted to contain HEAT repeats.[18] Despite the obvious similarities of Blm10 and PA200, published data present a confusing picture. Blm10 was initially identified as a factor important for repairing specific types of DNA damage,[17,19] and some features of mammalian PA200 are consistent with such a function.[10] A truncated fusion protein was found to be mislocalized and cells with this mutant protein were shown to be somewhat sensitive to the DNA damaging agent bleomycin, but deletion mutations did not share this sensitivity.[18] Recently, it was reported that PA200 is essential for spermatogenesis in mice.[20] It has also been shown that Blm10 interacts with nascent but not mature 20 S proteasomes and that it functions in the coordination of proteasome assembly in yeast.[16] Finally, yeast cells lacking the ability to upregulate proteasome subunit expression due to deletion of the *RPN4* gene have been reported to be more sensitive than normal to low levels of canavanine, consistent with a defect in processing misfolded proteins.[18] Thus, the physiological role(s) of PA200 and Blm10 and the extent to which the functional roles have been conserved throughout evolution remain uncertain.

Here, we report an efficient purification method able to yield abundant stable Blm10 complexes with mature yeast 20 S proteasomes that are stoichiometrically assembled and suitable for structural studies. This allowed us to obtain images of Blm10–20 S complexes by cryo-electron microscopy and to calculate a three-dimensional model of the yeast 20 S proteasome with a Blm10 molecule bound at each end. This extends the resolution of the structural model beyond that available from negatively stained samples.[18] The 3D-map shows that Blm10 binding to the ends of the 20 S proteasome opens the axial gates on the α rings in a manner similar to its mammalian homolog PA200. This result shows that both activators share a similar proteasome activation mechanism. Moreover, the map is consistent with the solenoid predicted by the presence of multiple HEAT-like repeats in the Blm10 sequence.[15] We also describe genetic experiments to investigate the role of Blm10 in DNA damage repair and in growth at high temperatures. In contrast to earlier reports,[17–19] our results do not support a significant role for Blm10 in DNA damage repair or resistance to stresses that cause misfolding of proteins.

## Results

### Purification of stable and active Blm10–20 S proteasome complexes

Recombinant N-terminally histidine-tagged Blm10 was expressed in yeast (*Saccharomyces cerevisiae*) and purified by nickel affinity chromatography. Incubation of Blm10 with yeast 20 S proteasome that was bound to IgG-Sepharose beads by a protein A affinity tag, resulted in formation of stable $Blm10_2$–20 S (doubly capped) complexes that were released from the beads by incubation with TEV protease (Figure 1(a) and (b)).

Blm10 is a single polypeptide chain of 2144 residues. It undergoes proteolytic cleavage upon storage to yield predominantly two large fragments visualized by SDS–PAGE. Each of the two large Blm10 fragments (Figure 1(a)) were shown by N-terminal sequencing to comprise at least two different starting points and represent roughly the N-terminal (N-terminally sequenced as $Asn^{188}$-AsnThrAlaGlu and $Gly^{228}$LysIleThrAla) and the C-terminal ($Ile^{1087}$GluAlaGly, $Ser^{1140}$AspLeuAlaPhe) halves of Blm10. Due to the broad appearance of these bands, it is likely that they comprise additional similar N-terminal and C-terminal fragments that were not detected by sequencing.

This clipping of Blm10 into covalently separated sections presumably occurs at exposed surface regions and does not appear to significantly alter the structure as judged by native gel analysis (Figure 1(b)). This is consistent with inspection of amino acid sequences; the N-terminal ~500 residues of Blm10 are poorly conserved and residues from ~1040 to 1140 lack counterparts in other species, suggesting that they form an exposed loop. It therefore seems likely that these regions can be processed without impacting structurally important interactions within Blm10 or between Blm10 and the 20 S proteasome.

Solutions of 20 S proteasome or Blm10–20 S complex that contain equal amounts of 20 S were tested for their ability to hydrolyze a fluorogenic peptide substrate (Figure 1(c) and 1(d)). We find that Blm10 stimulates hydrolysis of a peptide substrate approximately fourfold. This level of activation is lower than that reported for members of the PA28/11S family of proteasome activators,[21–23] but it is reproducible and it is seen both in gel overlay (Figure 1(c)) and in solution (Figure 1(d)) assays. The level of activation is essentially identical in one-day old preparations that show only slight proteolysis of Blm10 and in 21-day old preparations that show

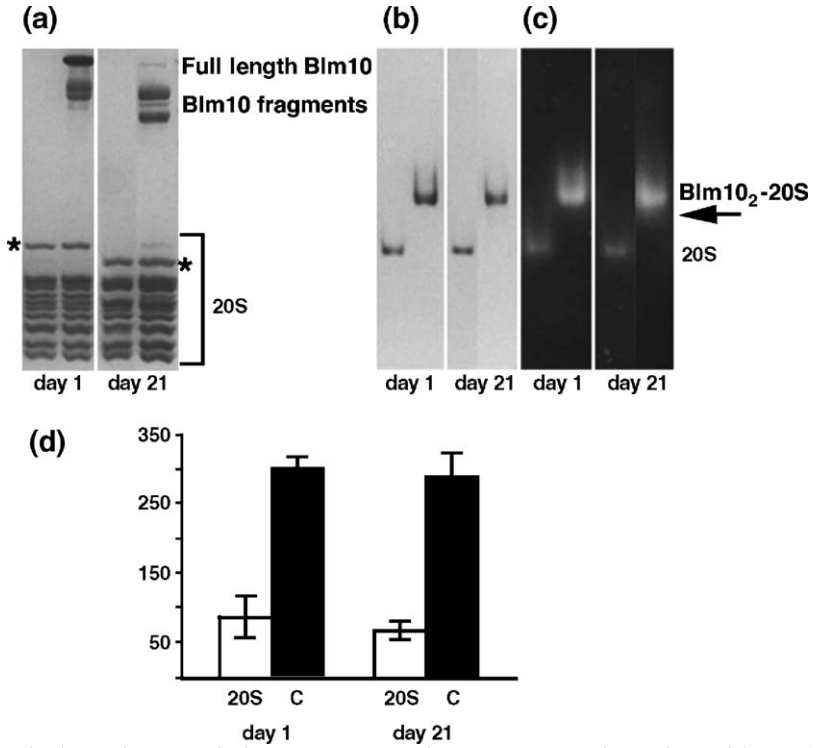


**Figure 1.** Analysis of active Blm10–20 S proteasome complexes. (a) Representative Blm10$_2$–20 S samples were compared by denaturing polyacrylamide gel (Coomassie) 1 and 21 days after completing the preparation. Upon storage of the purified complex at 4 °C, purified Blm10 becomes processed, predominantly to two large fragments that roughly correspond to the N and C-terminal halves of the protein. Asterisks indicate a proteasome 20 S subunit that also becomes processed during storage. (b) Native gel (Coomasie) analysis of the same samples indicates that the covalently separated products remain associated in a stable complex with 20 S proteasome. (c) Equivalent samples run in parallel developed using in-gel peptidase assays show approximately the same level of Blm10-mediated activation for one and 21 day-old complexes. Although not present in this sample, the position to which singly capped Blm10p–2 0S complexes migrate is also indicated (arrow). This assay was modified from a published method[43] using 4% non-denaturing gels run for 200 volt-hours in 0.5× Tris-Borate. The gel was incubated in 10 ml of 10 μm sLLVY-AMC substrate in assay buffer (20 mM sodium/potassium phosphate (pH 7.5), 50 mM NaCl, 1 mM DTT) for 30 min at 30 °C prior to visualization using a UVP BioDocIt system. (d) Solution assays also show equivalent rates of activation for complexes 1 and 21 days after preparation. This assay was optimized from a published method[21] to accommodate a 96 well format and a Polarstar Optima (BMG Labtech) fluorometer. 100 ng or 170 ng of double-headed complex in 90 μl of assay buffer were pre-incubated at 30 °C for 12 min prior to adding 10 μl of 1 mM sLLVY-AMC substrate for a final concentration of 100 μM. After addition of substrate, incubation at 30 °C was continued and fluorescence was read every 5 min for 1 h, then SDS was added to a final concentration of 0.01% and fluorescence was followed for another hour to verify that the 20 S was still capable of being activated (data not shown). Fluorescence/min was calculated using values within the linear range (CV = 1.0, $n = 6$ for each sample).

almost complete processing to the two major intermediate species. This further supports the conclusion that processing of Blm10 does not substantially alter the structure in the complex with 20 S proteasome.

## Cryo-electron microscopy of Blm10–20 S proteasome complexes

The purified complexes were analyzed by cryo-electron microscopy. Nearly 95% of the observed particles were oriented with the longitudinal axis parallel to the grid, as a consequence of pretreatment of the grids with polylysine.[24] This orientation made it possible to visually distinguish between Blm10$_2$–20 S (doubly capped) and Blm10–20 S (singly capped) complexes.

EM images most frequently showed Blm10$_2$–20 S complexes that contained the 20 S proteasome with a Blm10 molecule bound to each end (Figure 2). A smaller number of Blm10–20 S complexes were observed, as well as rare free 20 S proteasome particles.

These results further demonstrate that our purification method was very efficient at producing high yields of stable Blm10 complexes with mature 20 S proteasomes.

## Three-dimensional structure of the Blm10$_2$–20 S complex

Recent cryo-electron microscopy studies have shown that PA200 opens the axial channel of the

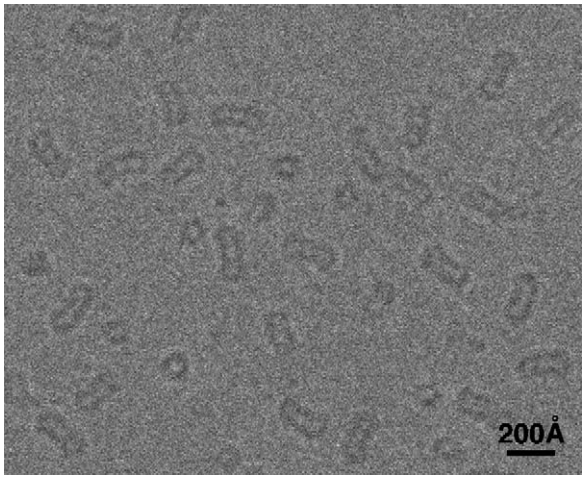


**Figure 2.** Cryo-electron microscopy of Blm10$_2$–20 S proteasome complexes. Representative micrograph of Blm10–20 S and Blm10$_2$–20 S proteasome complexes embedded in vitreous ice.

20 S proteasome upon binding to its ends in a fashion similar to that previously described for PA26.[8] To determine whether Blm10 protein activates the 20 S proteasome in similar fashion, we used cryo-EM to build a 3D model of the $Blm10_2$–20 S proteasome complex.

The reconstruction of the $Blm10_2$–20 S complex was calculated by the projection matching approach from several initial models and attempting many variations of the reconstruction process. Regardless of the initial map and the detailed protocol for the refinement process, we consistently obtained essentially the same final result. The resolution calculated for the refined 3D model was 18 Å.

The Euler angle distribution of aligned particle images within the asymmetric triangle revealed some degree of preferential orientation. The large initial number of particles used for the reconstruction (86,425) assured that most class averages contained at least 100 particle images and therefore, a complete description of the complex was obtained. However, the preferential orientation of the particles produced anisotropic resolution in the three-dimensional model with views described by over-represented projections showing slightly higher resolution than others (Figure 3(a) *versus* 3(b), respectively). The number of particles in over-populated projections was also limited to 400 particles to avoid over-representation of images in class averages, a problem that is difficult to compensate for with weighting factors used to place the class averages within a 3D Fourier volume. The number of particles incorporated in the final three-dimensional model was 47,567.

One molecule of Blm10 binds to each end of the yeast 20 S proteasome as an asymmetric cap (Figure 3). Viewed along the longitudinal axis, Blm10 showed the solenoid folding predicted by bioinformatics studies (Figure 4(a), left and center panels) and the thickness of the solenoid is very similar to the one observed in other HEAT repeat containing proteins such as karyopherin-β2[25] (Figure 4(a), center and right panels). The solenoid is bound to the α-ring, contacts each of the α subunits, and appears to spiral along the 7-fold pseudo-symmetry axis of the 20 S proteasome. This visualization of the solenoid structure bound to Blm10 is consistent with and extends the resolution of the 2D negative stain analysis by Schmidt *et al.*[18] Although no symmetry was applied during the construction of the model, Blm10 caps at both ends were very similar and had the same shape (Figure 3).

When the three-dimensional reconstruction was cut sagitally, the Blm10 caps featured a cavity that connects with the pre-chambers of the 20 S proteasome by an opening on the axial channel. The opening of the axial channel was evident both in a surface rendering representation (Figure 4(b)) and in a central section of the density map (Figure 4(c), left panel, white arrow). The center of both α rings clearly showed decreased density compared to a map of free 20 S obtained from the X-ray structure of the yeast proteasome[3] limited to 18 Å resolution (not shown). An internal control for our sample was provided by the contaminant particles representing the Blm10–20 S complex in our data set. A low-resolution three-dimensional reconstruction was obtained from these particles (~3500). In a sagital section, the Blm10-free end of the 20 S proteasome showed the same level of density all across the α ring, suggesting that the axial channel of the yeast 20 S proteasome is closed in solution when Blm10 is not bound (Figure 4(c), right panel, yellow arrow).

## Orientation of the 20 S proteasome in the Blm10–20 S proteasome complex

We determined the orientation of the 20 S proteasome within the map of the $Blm10_2$–20 S complex to identify the seven α subunits and define how Blm10 binds to the end of the proteasome. All α subunits in the yeast 20 S proteasome have a similar fold,[3] and we therefore needed to determine first whether we could distinguish them at the calculated resolution of our reconstructed map (18 Å). Our ability to distinguish the different α subunits at 18 Å was confirmed by comparing the 7-fold symmetrized and the non-symmetrized atomic structure of the yeast 20 S proteasome[3] limited at 10 Å resolution. Fourier shell correlation (FSC) between these two maps started to drop at about 28 Å resolution and it reached 0.7 at 13 Å (Figure 5) suggesting that these two maps are significantly different in this spatial frequency range.

To determine whether during the refinement the 20 S proteasome model in the complex either remained in the same orientation or rotated around its longitudinal axis, we calculated the cross-correlation coefficient between the $Blm10_2$–20 S complex density map and the X-ray crystal structure limited to 15 Å that was used as starting model. This calculation was performed for all the other six symmetry related orientations of the X-ray crystal structure and restricted to the 20 S part of the density map in the complex. The highest cross-correlation coefficient was obtained for the orientation of the 20 S in the starting model suggesting that the 20 S proteasome in the complex did not rotate during the refinement process and that the α subunits can be assigned directly from the starting model (Figure 3). An identical result was obtained when the X-ray crystal structure of the 20 S proteasome was limited to other resolutions such as 10 Å, 15 Å and 25 Å, indicating the robustness of the result. This experiment shows that Blm10 binds to the α ring in a defined orientation and in the symmetric complex both caps are bound identically to the α ring. Importantly, this experimentally determined orientation places the proteasome's 2-fold axis coincident with the 2-fold axis relating density of the two independent Blm10 molecules at either end of the proteasome complex.

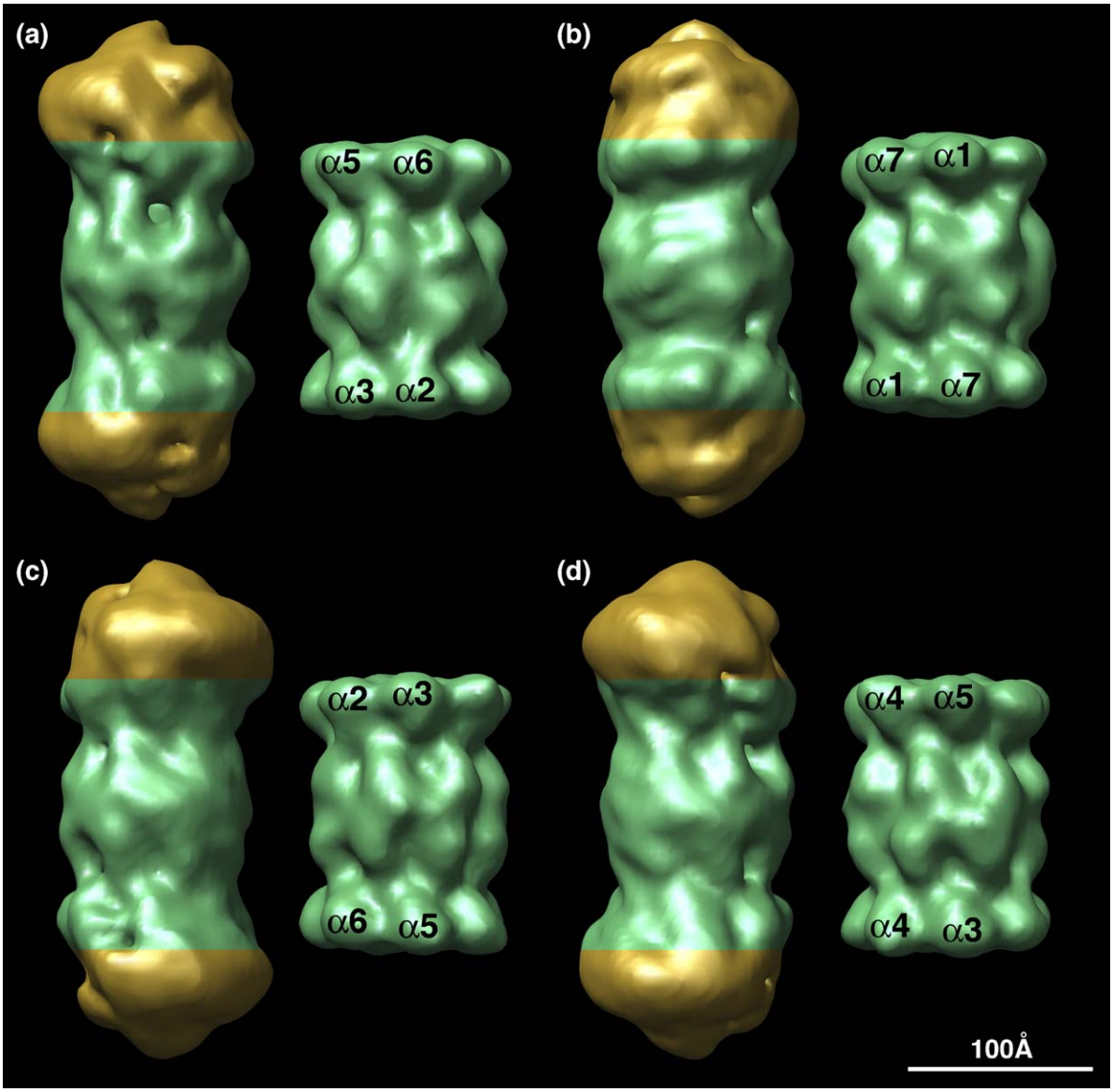


**Figure 3.** Three-dimensional reconstruction of the $Blm10_2$–20 S proteasome complex. Surface representation of the reconstruction of the $Blm10_2$–20 S proteasome complex at 18 Å resolution compared with the X-ray structure of yeast 20 S proteasome (PDB code,1RYP) limited at similar resolution. From (a) to (d) different side views of the complex are shown side-by-side with the analogous view of the 20 S proteasome. The contour used for the representation of the $Blm10_2$–20 S complex displays a molecular volume corresponding to a complex of 1.2 MDa. Blm10 is shown as the non-symmetrical caps (colored in light brown) bound to the ends of the proteasome (colored in green). The two molecules of Blm10 contact the α rings at both ends of the proteasome in the same manner. All the α subunits are contacted by Blm10.

### *BLM10* mutants are not sensitive to DNA damage conditions

Previous publications reported that *BLM10* plays a role in DNA repair and is required to support growth at elevated temperatures.[17,19,26] To examine the role of Blm10 in yeast, we deleted the gene and examined the resulting cells.

Surprisingly, deletion of *BLM10* in the A364a strain background had no effect on the rate of growth or viability when cells were challenged with DNA-damaging agents such as bleomycin or phleomycin (Figure 6(a)). The drugs were effective, as they severely restricted the growth of an isogenic strain with the *dna2-2* mutation, which causes sensitivity to a range of DNA-damaging agents (Figure 6(a)).[27,28] Ploidy can affect the repair strategies used by yeast cells, as homologous repair is more readily available in diploids. We therefore tested sensitivity to these drugs in a homozygous deletion diploid strain, but this strain was not more sensitive to bleomycin or phleomycin than a wild-type (WT) diploid strain. Deletion of *BLM10* did not cause sensitivity to other forms of DNA damage, including exposure to gamma-irradiation (Figure 6(b)), methyl methane sulfonate (MMS), UV irradiation, camptothecin, and hydroxyurea (not shown). These treatments caused inviability of sensitive control strains but the *blm10-Δ* mutant strain paralleled the growth rate and viability of the WT

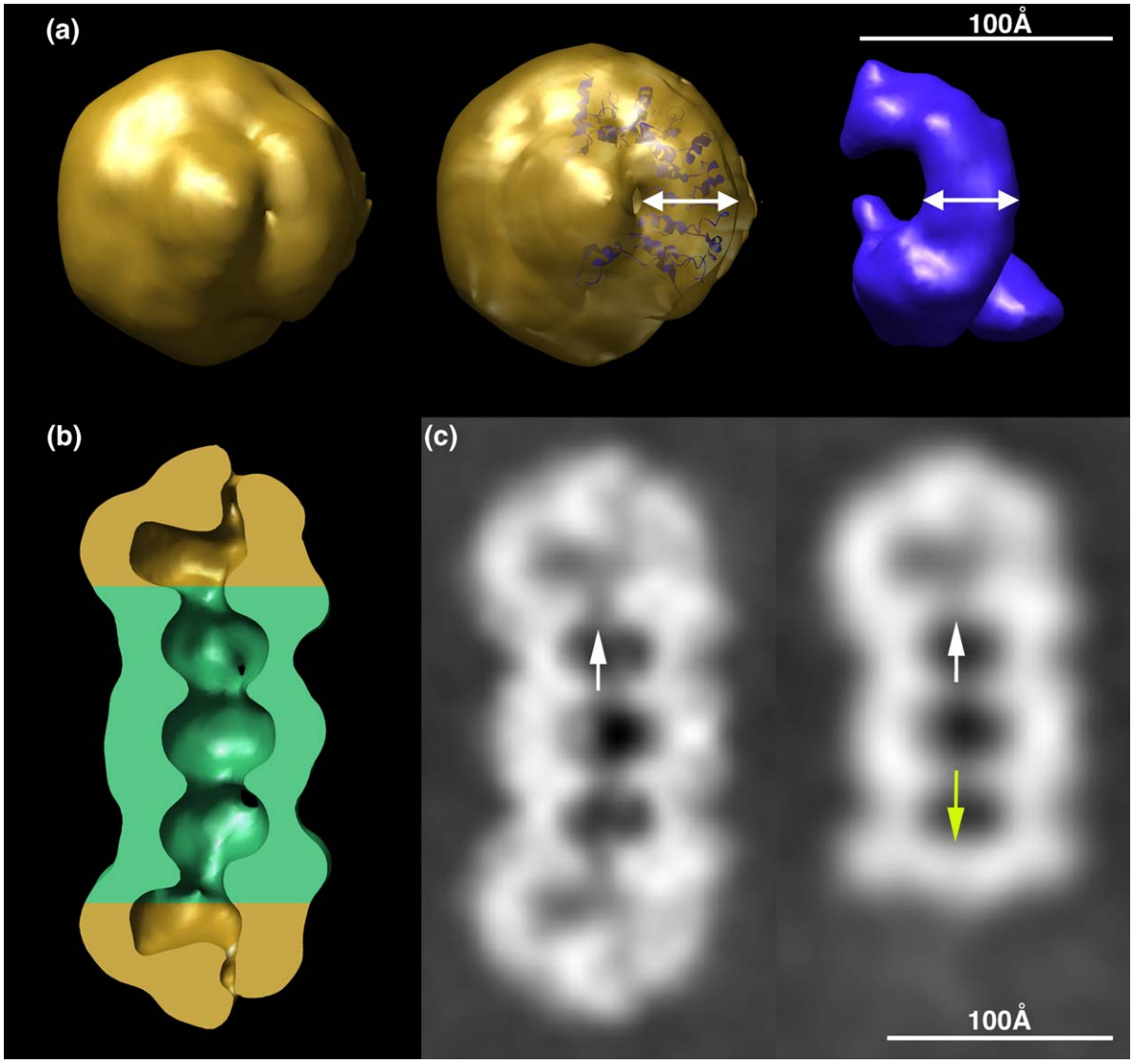


**Figure 4.** Visualization of the solenoid folding of the Blm10 protein. Opening of the proteasomal axial channel upon Blm10 binding. (a) Surface representation of the axial view of the two Blm10 caps in a $Blm10_2$–20 S proteasome complex (left and center panels) compared with the HEAT-repeat containing structure of karyopherin-β2 protein (PDB code,1QBK) blurred to 18 Å resolution (right panel). Double-headed arrows span the thickness of the solenoid in both proteins. Part of the atomic structure of karyopherin-β2 (residues Tyr3 to Leu394) was docked into the solenoid path of the Blm10 cap (center panel). (b) Sagital cut of the surface rendering representation of the $Blm10_2$–20 S proteasome complex. The light brown Blm10 caps at both ends of the 20 S proteasome feature an internal cavity communicated with the digestion chamber of the proteasome by an opening of the axial channel. (c) Central section of the density maps of the $Blm10_2$–20 S (left panel) and Blm10–20 S (right panel) complexes. Density in the center of the α rings in contact with Blm10 (white arrows) in both complexes is significantly lower than in the free α ring (yellow arrow) in the asymmetric complex.

control in all cases (Figure 6(b), and data not shown).

Meiosis involves extensive recombination between homologous chromosomes, thus mutations that cause defects in DNA damage repair often cause defects in sporulation in yeast. However, diploids lacking both copies of *BLM10* were able to form viable spores at rates qualitatively the same as WT, indicating normal ability to progress through the meiotic program in the absence of *BLM10* (not shown). Therefore, we conclude that *BLM10* is not needed for repair of various forms of DNA damage or to perform meiotic recombination.

Strains lacking *BLM10* also grew at normal rates at temperatures ranging from 13 °C to 38 °C (Figure 6(c), and data not shown), indicating that Blm10 is not needed for survival at extreme temperatures.

We performed additional controls to determine whether the previously observed phenotypes are dependent on the genetic background and the mating type of the strain tested. The same deletion allele was introduced into W303 and S288C strains and similar results to those described above were obtained in these backgrounds (not shown). No defects in DNA repair were observed in *MAT*a haploids, Matα haploids, or MATa/Matα diploids

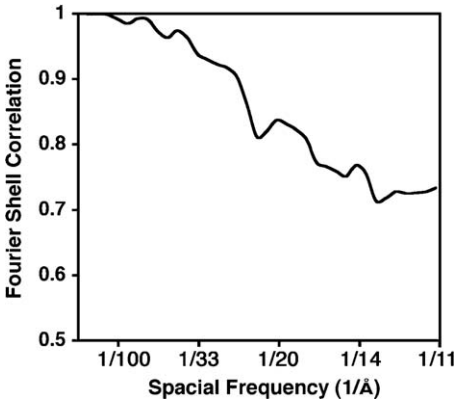


**Figure 5.** Spatial frequency range in which the seven α subunits of the 20 S proteasome can be differentiated. Comparison of the 20 S proteasome density map with a D7 symmetrized version to establish a spatial frequency range of significant difference for distinguishing the seven quasi-equivalent orientations. A 10 Å resolution 20 S proteasome map was generated from the X-ray structure (PDB code,1RYP), and D7 (dihedral 7-fold) symmetrized. The two maps were compared using Fourier shell correlation. The two maps differed at spatial frequencies beyond 30 Å. The orientation of the 20 S proteasome in the Blm10–20 S complex shown in Figure 3 by cross-correlation was done at 18 Å.

lacking *BLM10* (Figure 6(a) and (b), and data not shown). However, as previously reported, deletion of the gene encoding the DNA polymerase α binding protein Ctf4 used as a control, caused sensitivity to bleomycin and gamma irradiation specifically in strains expressing the *MATα* mating type allele[29] (Figure 6(a) and (b)). Therefore, the conclusion that *BLM10* is not needed to promote growth at extreme temperatures or for DNA damage repair seems to be independent of the genetic backgrounds and the mating type of the strain.

Finally, we attempted to reproduce the published results that seem to implicate *BLM10* in DNA damage repair, allowing growth at high temperatures, or surviving exposure to low levels of canavanine. We obtained strains from the standard BY4743 deletion collection affecting *BLM10*,[30] a background isogenic with the strains described by Schmidt *et al.*[18] Due to a sequencing error in the original genomic database release, *BLM10* was initially thought to be two open reading frames (ORFs), *YFL007w* and *YFL006w*.[26] Deletion of *YFL007w* removes the initiating methionine and about 80% of the *BLM10* ORF, while deletion of *YFL006w* should allow expression of a C-terminal truncation protein that is missing the most highly conserved region of *BLM10*. In our experiments, the BY4743 background was significantly more resistant to phleomycin than A364a strains, but neither deletion within the *BLM10* region affects growth at high temperatures or on media containing phleomycin (Figure 6(c)). Schmidt *et al.*[18] reported that a strain lacking both Blm10 and Ecm29 displayed increased sensitivity to the amino acid analog canavanine, but our results do not confirm this result (Supplementary Data). We did find that overexpression of Blm10 is detrimental to growth, and may have a slightly greater negative effect on media containing bleomycin, but these overexpression effects are likely to be indirect results of the sequestering of 20 S proteasomes (Supplementary Data). These results support the conclusion that *BLM10* is not needed for growth at high temperature or for various forms of DNA damage repair.

## Discussion

The sequence conservation between mammalian PA200 and yeast Blm10 suggested that they are functional homologs. This assumption has been obscured, however, by apparently conflicting functional data.[10,16,18] The 23 Å resolution reconstruction of bovine PA200 in complex with bovine 20 S proteasome has been reported,[14] and Blm10 also binds to the ends of mature proteasomes and stimulates their peptidase activity.[18] Efforts to advance structural studies have been hindered by the low natural abundance and difficulty in separating Blm10 complexes from other activated proteasomes. We therefore developed an efficient purification method for the $Blm10_2$–20 S complex. The high yield of complexes obtained facilitated the higher resolution reconstruction reported here, and further established the structural and biochemical relationship between yeast Blm10 and mammalian PA200.

The structural similarity is shown by comparing the previously described 3D-reconstruction of the bovine PA200–20 S complex[14] with the one from yeast Blm10–20 S complex described here. This comparison reveals significant similarities between both models including the observation that both PA200 and Blm10 proteins bind to the ends of the proteasome as hollow asymmetric caps (Figure 7(a)) and that both proteins cause opening of the axial channel, further suggesting a conserved mechanism for activation of the 20 S proteasome.

Some interesting differences are also observed. For example, the Blm10 solenoid appears to be tightly packed and to contact all of the α subunits, whereas PA200 features an opening in its surface as it does not contact the α7 subunit in the 20 S proteasome[14] (Figure 7(b)). The absence of large openings in the surface of Blm10 raises the question of how peptides can access or exit the digestion chamber once the Blm10 cap is bound to the α ring. Because Blm10–20 S proteasome complexes are labile and dynamic,[18] one possibility is that Blm10 binds substrates before docking onto the 20 S proteasome ends, whereupon Blm10 would open the gate of the axial channel and substrates diffuse into the digestion chamber. Alternatively, our reconstruction shows a narrow entrance pore in the Blm10 cap close to the

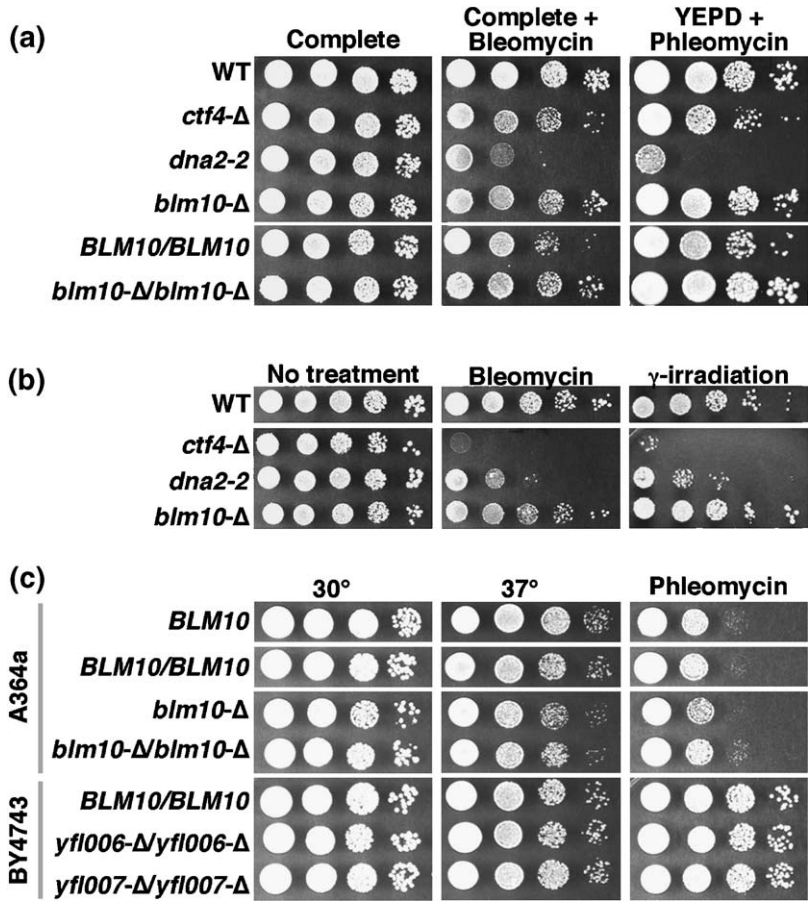


**Figure 6.** Deletion of *blm10* does not cause sensitivity to DNA damage or high temperature. (a) Cultures of haploid yeast strains from the A364a strain background 4053-5-2 (WT), 7883-6-3 (*ctf4-Δ*), 7757-3-3 (*dna2-2*), 8015-4-1 (*blm10-Δ*), or diploids 7860 (WT), and 8052 (*blm10-Δ/blm10-Δ*) (Table 2) were grown to saturation in rich medium. Aliquots of tenfold serial dilutions were spotted to complete synthetic medium, complete medium with 12 μg/ml bleomycin (Sigma), or rich medium with 8 μg/ml phleomycin (Sigma), then incubated at 30 °C. (b) Cultures were grown and processed as for (a), except strains 7860-6-3 (WT), 7373-1-4 (*ctf4-Δ*), 7757-6-3 (*dna2-2*), and 8015-4-3 (*blm10-Δ*) with the *MAT*α mating type allele were used (Table 2). The plate in the right panel was exposed to about 100 kRad of gamma-irradiation from a $Cs^{137}$ source after cells were placed on the plate. (c) Cultures of the A364a strains 4053-5-2 (WT, haploid), 7860 (WT, diploid), 8015-4-1 (*blm10-Δ* haploid), and 8052 (*blm10-Δ/blm10-Δ* diploid), or the diploid BY4743 (Table 2) and its isogenic derivatives with deletions of *YFL006w* or *YFL007w* obtained from Research Genetics[30] were processed as for (a), then incubated on rich medium at 30 °C, 37 °C, or on rich medium containing 8 μg/ml phleomycin at 30 °C. Incubation of all plates was terminated when the more phleomycin resistant BY4743 (Table 2) strains grew to full size, so the A364a strains appear to be more sensitive to phleomycin here than in (a).

longitudinal axis. This pore could expand under certain conditions and allow the traffic of peptides. Another possibility is that some portion of the Blm10 structure is sufficiently flexible to allow passage of peptides yet also sufficiently occupied to display significant density in our reconstructions. "Flexible curtains" of this nature appear to be present at the axial opening of archaeal 20 S proteasomes[2] and in a central loop of the PA26 activator.[6]

The original *blm3-1* mutation which was reported to be suppressed by *BLM10* caused sensitivity to gamma-irradiation and to the oxidizing agent hydrogen peroxide.[19] Moreover, a deletion of the N-terminal region of *BLM10* was reported to cause sensitivity to phleomycin.[17,19,26] These results suggested that Blm10 functions in DNA repair. Subsequently, *BLM10* deletion was found to make growth of yeast strains temperature sensitive.[16] In apparent conflict with these reports, our genetic data indicate that *BLM10* is not needed for repair of various forms of DNA damage or for survival at extreme temperatures. Furthermore, our results are consistent with published data from a number of high throughput screens that have been performed using the standard BY4743 deletion collection or isogenic relatives,[30] none of which have revealed phenotypes caused by the *yfl006w* or *yfl007w* deletions. Therefore, although conservation of sequence, structure, and proteasome activation argue strongly for a conserved function of Blm10 and PA200, the actual physiological role remains obscure. Definition of the functional roles and the extent to which they

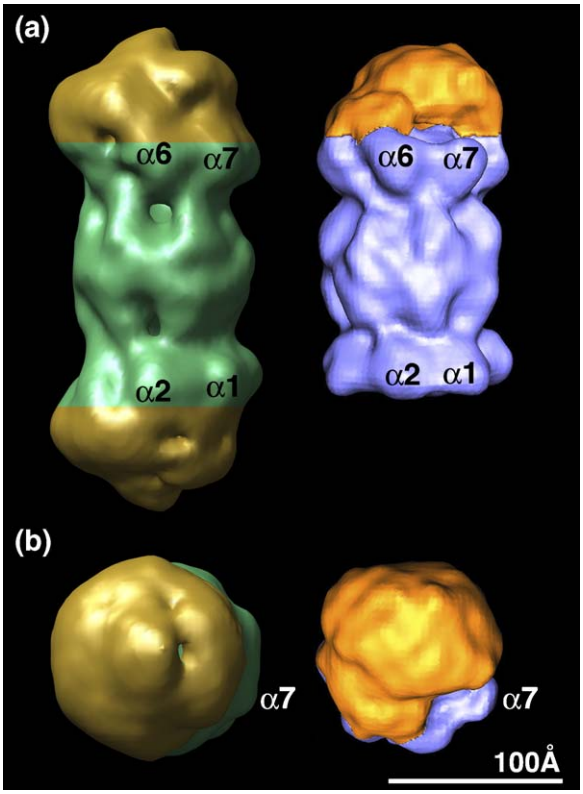


**Figure 7.** Comparison of the three-dimensional reconstruction of the yeast $Blm10_2$–20 S and bovine PA200–20 S proteasome complexes. Two analogous views of the surface representation of yeast $Blm10_2$–20 S proteasome (left) and bovine PA200–20 S[14] complexes (right). View perpendicular (a) to and along (b) the longitudinal axis.

overlap for PA200 and Blm10 remain important questions for future studies.

## Materials and Methods

### Construction of BLM10 plasmid to overexpress the protein in yeast cells

Due to the large size of *BLM10*, a gap repair strategy was used to construct a plasmid to overexpress the protein in yeast cells. The 681 bp BamHI-EcoRI fragment containing the *GAL1-GAL10* promoter region from pMTL[31] was inserted into YEplac195.32 This was digested with BamHI and HindIII and two overlapping oligos (PA-10 and PA-11; Table 1) were annealed and inserted to make pTF153. Primers PA-06 and PA-09 (Table 1) were used to amplify a 227 bp fragment containing the 5′ end of the *BLM10* ORF by PCR, and primers PA-07 and PA-08 (Table 1) were used to amplify a 574 bp fragment containing the 3′ end of the ORF and extending 448 bp downstream of it. The two fragments were digested with KpnI and BamHI or BamHI and XhoI, respectively, then ligated with pTF153 digested with KpnI and XhoI to produce pTF155i. After digestion with BamHI, the linearized pTF155i with 223 bp of homology to the 5′ end of *BLM10* and 549 bp of homology to the 3′ flanking region was used to transform the FY2/S288C strain BY4743 (Table 2).[30] Plasmids which had repaired the 6083 bp gap to reconstitute the *BLM10* ORF under control of the *GAL1* promoter and with 12 histidine residues fused to the N terminus were recovered. The initiating methionine of the 2143 residue *BLM10* ORF is replaced with $MH_{12}G$... in this construct, making a protein of 2157 residues. Sequencing confirmed the accuracy of the construction and the gap repair.

### Preparation of Blm10–20 S proteasome complex

N-terminally 12X-histidine tagged Blm10 protein was recombinantly expressed in the yeast (*S. cerevisiae)* strain Bcy213 (Table 2). Cells were grown to an optical density (600 nm) of ~0.7 in synthetic medium containing 2% (w/v) raffinose, 1.3 g/l amino acid $mix^{-URA}$, and 1% (w/v) ammonium sulfate. Expression of Blm10 was induced by addition of 20% (w/v) galactose to the culture to a final concentration of ~1.1%. Cells were harvested by centrifugation 12–18 h after induction, washed with $dH_2O$, resuspended in a volume of $dH_2O$ equal to the pellet weight and flash frozen in liquid nitrogen. With the exception of weighing/thawing and cell disruption, all subsequent steps were performed at 4 °C.

Typical preparations started with 80 g of frozen cell paste, which were thawed and added to an equal volume of 2× lysis buffer to a final concentration of 20 mM Tris (pH 7.5), 1 M NaCl, 5 mM β-mercaptoethanol, 1 mM EDTA, 0.1% (v/v) NP40, 20 mM imidazole, and protease inhibitors (leupeptin 0.5 μg/ml, pepstatinA 0.7 μg/ml, aprotinin 0.5 μg/ml, and PMSF 0.25 mg/ml added during the lysis step). Cells were disrupted using a Gaulin homogenizer, the lysate clarified by centrifugation, and batch-bound for 1 h to 10 ml of Ni-NTA slurry equilibrated with 20 mM Tris (pH 7.5), 50 mM NaCl, 50 mM imidazole, and 0.01% NP40. The resin was packed into a column and washed with 50 ml of 20 mM Tris (pH 7.5), 2 M NaCl, 50 mM imidazole, 0.01% NP40 followed by 50 ml of 20 mM Tris (pH 7.5), 50 mM NaCl, 50 mM imidazole,

**Table 1.** Oligonucleotide primers used

| | |
|---|---|
| PA-01 | GCGCGGTACCTCTGCTATAACCCGTC |
| PA-02 | GCGCGAATTCATTGGCGGTAACAAATCG |
| PA-03 | GCGCGGATCCGAAGTTACTATGCCTGATTC |
| PA-04 | GCGCGGTACCAGGTTGGAATAATGGATCAC |
| PA-06 | GAAGTGGGATCCATGCCATTGAACAG |
| PA-07 | GCGCGGATCCCTATTAGTGAGTTCAAGAAG |
| PA-08 | GAAACAGTTCTCGAGCCTGACATGTTTATC |
| PA-09 | GCCAGGTACCGCTAACAATGACGATGA |
| PA-10 | GATCGACATGCATCACCACCATCATCACCACCATCATCATCACCATGGTACCGGATCCGTCGACCTGCAGCTCGAG |
| PA-11 | AGCTCTCGAGCTGCAGGTCGACGGATCCGGTACCATGGTGATGATGATGGTGGTGATGATGGTGGTGATGCATGTC |

All primers are shown 5′ to 3′.

**Table 2.** Yeast strains used

| | |
|---|---|
| 4053-5-2 | *MATa trp1 leu2 ura3 his7* |
| 7373-1-4 | *MATα trp1 leu2 ura3 his3 ctf4-Δ(::TRP1)* |
| 7757-3-3 | *MATa trp1 leu2 ura3 his7 dna2-2* |
| 7757-6-3 | *MATα trp1 leu2 ura3 his3 dna2-2* |
| 7860 | *MATa/MATα ura3-Δ0/ura3-Δ0 leu2-Δ0/leu2-Δ0 trp1-Δ2/trp1-Δ2 his3/+ +/his7* |
| 7860-6-3 | *MATα ura3-Δ0 leu2-Δ0 trp1-Δ2 his3* |
| 7883-6-3 | *MATa trp1 leu2 ura3 his7 ctf4-Δ (::TRP1)* |
| 8015-4-1 | *MATa ura3-Δ0 leu2-Δ0 trp1-Δ2 his7 blm10-Δ(::TRP1)* |
| 8015-4-3 | *MATα ura3-Δ0 leu2-Δ0 trp1-Δ2 his3 blm10-Δ(::TRP1)* |
| 8052 | *MATa/MATα ura3-Δ0/ura3-Δ0 leu2-Δ0/leu2-Δ0 trp1-Δ2/trp1-Δ2 his3/+ +/his7 blm10-Δ(::TRP1)/blm10-Δ(::TRP1)* |
| BY4743 | *MATa/MATα leu2-Δ0/leu2-Δ0 ura3-Δ0/ura3-Δ0 his3-Δ1/his3-Δ1 met15-Δ0/+ +/lys2-Δ0* |
| BCY213 | *MATa pep4-Δ(::HIS3) prb-Δ(::LEU2) bar1-Δ(::HISG) lys2-Δ(::GAL1/10-GAL4) can1 ade2 trp1 ura3 his3 leu2-3,112* |

All strains are isogenic with A364a except BY4743.[30]

0.01% NP40. Blm10 was eluted with 100 ml of 20 mM Tris (pH 7.5), 50 mM NaCl, 500 mM imidazole, 0.01% NP40. The eluted solution was collected into fresh β-mercaptoethanol to yield a final β-mercaptoethanol concentration of 5 mM.

Blm10–proteasome complex was prepared using yeast strain SDL135 in which the genomic copy of the Pre1 (β4) subunit gene encodes a domain of protein A at its C terminus.[33] About 80 g of frozen cell pellets (expressing Pre1-protein A 20 S) were prepared and bound to 10 ml IgG-Sepharose resin as described.[34] The immobilized 20 S proteasome was equilibrated with 50 mM Tris (pH 7.5), 1 mM EDTA and all of the Blm10 previously eluted from Ni-Nita resin (typically 10–50 mg of Blm10) was incubated with 20 S-IgG for 1 h. Blm10–20 S complex (bound to IgG) was washed first with 500 ml of 50 mM Tris (pH 7.5), 1 mM EDTA, and second with 500 ml of 50 mM Tris (pH 7.5), 1 mM EDTA, 100 mM NaCl. The resin was collected into a glass column and washed with 20 ml of 50 mM Tris (pH 7.5), 1 mM EDTA, 50 mM NaCl, 0.5 mM dithiothreitol. The Blm10–20 S complex was released from the IgG resin with TEV protease at a final concentration of 2–8 μg/ml in 20 ml of 50 mM Tris (pH 7.5), 1 mM EDTA, 50 mM NaCl, and 0.5 mM dithiothreitol overnight. The purified Blm10–20 S complex was collected by draining the column and washing with an additional 20 ml of TEV buffer. The protein was concentrated in a spin filtration device and dialyzed against 20 mM Tris (pH 7.5), 25 mM KCl, 10 mM NaCl, 1 mM $MgCl_2$, 0.1 mM EDTA, 1 mM dithiothreitol, and 0.5% (v/v) glycerol for EM and SAXS analysis.

## Cryo-electron microscopy

Freshly prepared holey carbon grids (400 mesh copper) were washed with acetone for 15 min and their surface was glow discharged in air for 30 s.[35] Grids were then floated on a five μl drop of polylysine hydrobromide (0.1% (w/v) aqueous solution; $M_r$ 60–120 kDa; Polysciencies, Inc) for 2 min. Excess polylysine solution was blotted away and a 3.5 μl drop of sample at a protein concentration of 100 μg/ml was deposited on the grid. After blotting, the grid was plunged into liquid ethane and transferred to a Philips CM200 FEG electron microscope operated at 120 kV with a Gatan 626 cryo-holder. Focal pair images were acquired with low-dose techniques using nominal defocus values between 0.9 μm and 2.1 μm and 38,000× magnification. Kodak SO-163 film was used to record the images and they were digitized with a SCAI scanner (Z/I Imaging, Huntsville, AL) and binned twofold giving a sampling of 3.68 Å/pixel. Only images showing no drifting or astigmatism and with visible Thon rings in the power spectrum up to at least 12 $Å^{-1}$ were used for the image processing.

## Three-dimensional reconstruction and visualization of maps

The program Boxer (EMAN)[36] was used to interactively pick 86,425 particles.

A rotationally averaged power spectrum was obtained from particles of each micrograph and used to determine the contrast transfer function (CTF) and envelope function parameters of the micrograph with ctfit (EMAN).[36] In this process an X-ray scattering profile of the $Blm10_2$–20 S complex was used (see Supplementary Data). CTF-phase flipping was performed directly on the particle images and amplitude correction for the CTF was done during the generation of class-averages.[37]

A total of 86,425 projection images representing side views (with the longitudinal axis parallel to the grid) were selected. Only side views were selected, since these views enable us to visually distinguish whether Blm10 was bound to either one or both ends of the 20 S proteasome. This set of views completely covers the Fourier space and provides all of the necessary information to build an accurate 3D model.

Orientations of the particles were determined by the projection matching approach provided by EMAN. Sets of projections were calculated from the initial maps using an angular spacing of 4.3° and particles were classified by comparison to these projections. After two cycles of refinement the resulting map was used to produce a Blm10–20 S complex with a cap only on one end. These $Blm10_2$–20 S and Blm10–20 S models were used for a classification step in which projections from different view angles were calculated from both maps and each particle image was cross-correlated to projections from both maps. Particles assigned to the Blm10–20 S map were discarded and the refinement continued with the particles assigned to the $Blm10_2$–20 S map. This classification step allowed us to eliminate the particles in our data set representing Blm10–20 S complexes that were erroneously picked. Convergence of the reconstruction was obtained upon four or five refinement cycles and symmetry was not imposed at any stage.

Non-model bias of the 3D-reconstruction was proven by using several initial maps including the symmetrized and non-symmetrized X-ray crystal structure of the yeast 20 S proteasome (PDB code, 1RYP) and crystal structure of PA26 from *Trypanosome Brucei* in complex with yeast 20 S proteasome (PDB code, 1FNT).[8] Both structures were limited at 15 Å resolution.

The correct handedness of the model was imposed by the yeast 20 S proteasome X-ray crystal structure[3] used as starting model because it cannot be determined from our untilted images.

Orientation determination of the 20 S proteasome in the symmetric Blm10–20 S complex was performed with the Foldhunter program.[38]

Resolution of the final map was estimated by two methods. First, the data set was split in two halves and a

3-D reconstruction was calculated from both halves independently using the same starting model and following the same refinement approach. Then Fourier shell correlation (FSC) was calculated between both maps applying the 0.5 FSC threshold. Second, we performed the even–odd test in EMAN[37,39] in which two maps were obtained following the last cycle of refinement from the even and odd numbered particles and compared by FSC.

The program Chimera[40,41] was used to generate surface rendering representations of the model and the rendering threshold selected included 100% of the mass of the complex. The Bshow program from the Bsoft package[42] was used to visualize the density maps.

### Deletion of *BLM10*

*BLM10* was deleted by amplifying fragments from the 5′ and 3′ flanks of the gene using PCR with primers PA-01 and PA-02 (digested with KpnI and EcoRI) and PA-03 and PA-04 (digested with KpnI and BamHI), respectively (Table 1). These were ligated with YIplac204,[32] digested with EcoRI and BamHI, and the product (pTF156) was digested with KpnI. Transformation of yeast strains with linearized pTF156 leads to replacement of the *BLM10* ORF with YIplac204 (*TRP1*), leaving only the first four and the last 14 bases of the 6429 bp ORF intact. Accuracy of the PCR products was confirmed by sequencing, and accuracy of integration was confirmed by Southern blotting.

## Acknowledgements

We are grateful to Alasdair Steven and the National Institutes of Health for the use of their microscopes and to Daniel Finley and David Legett for providing the yeast strain sDL135 that expresses the protein A-tagged Pre1 20 S subunit. We thank Susan Ruone and Shannon McCullock for assistance with the genetic analysis of Blm10 and Ecm29. We also thank Alasdair Steven, Martin Rechsteiner and John Rubinstein for insightful comments on the manuscripts. We are grateful to Steve Ludtke for advice with EMAN program and to Anita Orendt, Mike Malott and Todd Pfaff for computer support. This work was supported by grants from the Canadian Institutes of Health Research (CIHR), Canada Foundation for Innovation (CFI), Ontario Innovation Trust (OIT) and by NIH grant GM59135. J.O. is recipient of a CIHR salary award. Use of the Advanced Photon Source was supported by the US Department of Energy under contract no. W-31-109-ENG-38. 18ID beamline is a Research Center supported by the US National Institutes of Health under grant RR-08630.

## Supplementary Data

Supplementary data associated with this article can be found, in the online version, at doi:10.1016/j.jmb.2006.08.010

## References

1. Unno, M., Mizushima, T., Morimoto, Y., Tomisugi, Y., Tanaka, K., Yasuoka, N. & Tsukihara, T. (2002). The structure of the mammalian 20S proteasome at 2.75 Å resolution. *Structure (Camb)*, **10**, 609–618.
2. Lowe, J., Stock, D., Jap, B., Zwickl, P., Baumeister, W. & Huber, R. (1995). Crystal structure of the 20S proteasome from the archaeon T. acidophilum at 3.4 Å resolution. *Science*, **268**, 533–539.
3. Groll, M., Ditzel, L., Lowe, J., Stock, D., Bochtler, M., Bartunik, H. D. & Huber, R. (1997). Structure of 20S proteasome from yeast at 2.4 Å resolution. *Nature*, **386**, 463–471.
4. Voges, D., Zwickl, P. & Baumeister, W. (1999). The 26S proteasome: a molecular machine designed for controlled proteolysis. *Annu. Rev. Biochem.* **68**, 1015–1068.
5. Walz, J., Erdmann, A., Kania, M., Typke, D., Koster, A. J. & Baumeister, W. (1998). 26S proteasome structure revealed by three-dimensional electron microscopy. *J. Struct. Biol.* **121**, 19–29.
6. Forster, A., Masters, E. I., Whitby, F. G., Robinson, H. & Hill, C. P. (2005). The 1.9 Å structure of a proteasome-11S activator complex and implications for proteasome-PAN/PA700 interactions. *Mol. Cell*, **18**, 589–599.
7. Knowlton, J. R., Johnston, S. C., Whitby, F. G., Realini, C., Zhang, Z., Rechsteiner, M. & Hill, C. P. (1997). Structure of the proteasome activator REGalpha (PA28alpha). *Nature*, **390**, 639–643.
8. Whitby, F. G., Masters, E. I., Kramer, L., Knowlton, J. R., Yao, Y., Wang, C. C. & Hill, C. P. (2000). Structural basis for the activation of 20S proteasomes by 11S regulators. *Nature*, **408**, 115–120.
9. Hill, C. P., Masters, E. I. & Whitby, F. G. (2002). The 11S regulators of 20S proteasome activity. *Curr. Top. Microbiol. Immunol.* **268**, 73–89.
10. Ustrell, V., Hoffman, L., Pratt, G. & Rechsteiner, M. (2002). PA200, a nuclear proteasome activator involved in DNA repair. *EMBO J.* **21**, 3516–3525.
11. Kopp, F., Dahlmann, B. & Kuehn, L. (2001). Reconstitution of hybrid proteasomes from purified PA700-20 S complexes and PA28alphabeta activator: ultrastructure and peptidase activities. *J. Mol. Biol.* **313**, 465–471.
12. Hendil, K. B., Khan, S. & Tanaka, K. (1998). Simultaneous binding of PA28 and PA700 activators to 20 S proteasomes. *Biochem. J.* **332**, 749–754.
13. Cascio, P., Call, M., Petre, B. M., Walz, T. & Goldberg, A. L. (2002). Properties of the hybrid form of the 26S proteasome containing both 19S and PA28 complexes. *EMBO J.* **21**, 2636–2645.
14. Ortega, J., Bernard Heymann, J., Kajava, A. V., Ustrell, V., Rechsteiner, M. & Steven, A. C. (2005). The axial channel of the 20S proteasome opens upon binding of the PA200 activator. *J. Mol. Biol.* **346**, 1221–1227.
15. Kajava, A. V., Gorbea, C., Ortega, J., Rechsteiner, M. & Steven, A. C. (2004). New HEAT-like repeat motifs in proteins regulating proteasome structure and function. *J. Struct. Biol.* **146**, 425–430.
16. Fehlker, M., Wendler, P., Lehmann, A. & Enenkel, C. (2003). Blm3 is part of nascent proteasomes and is involved in a late stage of nuclear proteasome assembly. *EMBO Rep.* **4**, 959–963.
17. Febres, D. E., Pramanik, A., Caton, M., Doherty, K., McKoy, J., Garcia, E. *et al.* (2001). The novel BLM3 gene encodes a protein that protects against lethal effects of oxidative damage. *Cell. Mol. Biol. (Noisy-le-grand)*, **47**, 1149–1162.
18. Schmidt, M., Haas, W., Crosas, B., Santamaria, P. G.,

Gygi, S. P., Walz, T. & Finley, D. (2005). The HEAT repeat protein Blm10 regulates the yeast proteasome by capping the core particle. *Naure Struct. Mol. Biol.* **12**, 294–303.
19. Moore, C. W. (1991). Further characterizations of bleomycin-sensitive (blm) mutants of Saccharomyces cerevisiae with implications for a radiomimetic model. *J. Bacteriol.* **173**, 3605–3608.
20. Khor, B., Bredemeyer, A. L., Huang, C. Y., Turnbull, I. R., Evans, R., Maggi, L. B., Jr *et al.* (2006). Proteasome activator PA200 is required for normal spermatogenesis. *Mol. Cell. Biol.* **26**, 2999–3007.
21. Masters, E. I., Pratt, G., Forster, A. & Hill, C. P. (2005). Purification and analysis of recombinant 11S activators of the 20S proteasome: *Trypanosoma brucei* PA26 and human PA28 alpha, PA28 beta, and PA28 gamma. *Methods Enzymol.* **398**, 306–321.
22. Ma, C. P., Slaughter, C. A. & DeMartino, G. N. (1992). Identification, purification, and characterization of a protein activator (PA28) of the 20 S proteasome (macropain). *J. Biol. Chem.* **267**, 10515–10523.
23. Dubiel, W., Ferrell, K., Pratt, G. & Rechsteiner, M. (1992). Subunit 4 of the 26 S protease is a member of a novel eukaryotic ATPase family. *J. Biol. Chem.* **267**, 22699–22702.
24. Ortega, J., Singh, S. K., Ishikawa, T., Maurizi, M. R. & Steven, A. C. (2000). Visualization of substrate binding and translocation by the ATP-dependent protease, ClpXP. *Mol. Cell.* **6**, 1515–1521.
25. Chook, Y. M. & Blobel, G. (1999). Structure of the nuclear transport complex karyopherin-beta2-Ran X GppNHp. *Nature*, **399**, 230–237.
26. Doherty, K., Pramanik, A., Pride, L., Lukose, J. & Moore, C. W. (2004). Expression of the expanded YFL007w ORF and assignment of the gene name BLM10. *Yeast*, **21**, 1021–1023.
27. Budd, M. E. & Campbell, J. L. (2000). The pattern of sensitivity of yeast dna2 mutants to DNA damaging agents suggests a role in DSB and post-replication repair pathways. *Mutat. Res.* **459**, 173–186.
28. Formosa, T. & Nittis, T. (1999). Dna2 mutants reveal interactions with Dna polymerase alpha and Ctf4, a Pol alpha accessory factor, and show that full Dna2 helicase activity is not essential for growth. *Genetics*, **151**, 1459–1470.
29. Bennett, C. B., Lewis, L. K., Karthikeyan, G., Lobachev, K. S., Jin, Y. H., Sterling, J. F. *et al.* (2001). Genes required for ionizing radiation resistance in yeast. *Nature Genet.* **29**, 426–434.
30. Brachmann, C. B., Davies, A., Cost, G. J., Caputo, E., Li, J., Hieter, P. & Boeke, J. D. (1998). Designer deletion strains derived from *Saccharomyces cerevisiae* S288C: a useful set of strains and plasmids for PCR-mediated gene disruption and other applications. *Yeast*, **14**, 115–132.
31. Chang, Y. C. & Timberlake, W. E. (1993). Identification of *Aspergillus* brlA response elements (BREs) by genetic selection in yeast. *Genetics*, **133**, 29–38.
32. Gietz, R. D. & Sugino, A. (1988). New yeast-*Escherichia coli* shuttle vectors constructed with in vitro mutagenized yeast genes lacking six-base pair restriction sites. *Gene*, **74**, 527–534.
33. Leggett, D. S., Glickman, M. H. & Finley, D. (2005). Purification of proteasomes, proteasome subcomplexes, and proteasome-associated proteins from budding yeast. *Methods Mol. Biol.* **301**, 57–70.
34. Leggett, D. S., Hanna, J., Borodovsky, A., Crosas, B., Schmidt, M., Baker, R. T. *et al.* (2002). Multiple associated proteins regulate proteasome structure and function. *Mol. Cell.* **10**, 495–507.
35. Aebi, U. & Pollard, T. D. (1987). A glow discharge unit to render electron microscope grids and other surfaces hydrophilic. *J. Electron Microsc. Tech.* **7**, 29–33.
36. Ludtke, S. J., Baldwin, P. R. & Chiu, W. (1999). EMAN: semiautomated software for high-resolution single-particle reconstructions. *J. Struct. Biol.* **128**, 82–97.
37. Ludtke, S. J., Jakana, J., Song, J. L., Chuang, D. T. & Chiu, W. (2001). A 11.5 A single particle reconstruction of GroEL using EMAN. *J. Mol. Biol.* **314**, 253–262.
38. Jiang, W., Baker, M. L., Ludtke, S. J. & Chiu, W. (2001). Bridging the information gap: computational tools for intermediate resolution structure interpretation. *J. Mol. Biol.* **308**, 1033–1044.
39. Ludtke, S., He, K. & Huang, H. (1995). Membrane thinning caused by magainin 2. *Biochemistry*, **34**, 16764–16769.
40. Goddard, T. D., Huang, C. C. & Ferrin, T. E. (2005). Software extensions to UCSF chimera for interactive visualization of large molecular assemblies. *Structure (Camb)*, **13**, 473–482.
41. Pettersen, E. F., Goddard, T. D., Huang, C. C., Couch, G. S., Greenblatt, D. M., Meng, E. C. & Ferrin, T. E. (2004). UCSF Chimera—A visualization system for exploratory research and analysis. *J. Comput. Chem.* **25**, 1605–1612.
42. Heymann, J. B. (2001). Bsoft: image and molecular processing in electron microscopy. *J. Struct. Biol.* **133**, 156–169.
43. Bajorek, M., Finley, D. & Glickman, M. H. (2003). Proteasome disassembly and downregulation is correlated with viability during stationary phase. *Curr. Biol.* **13**, 1140–1144.

***Edited by W. Baumeister***

*(Received 25 May 2006; accepted 4 August 2006)*
Available online 9 August 2006

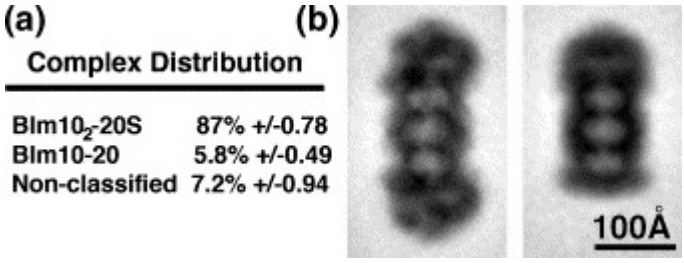


Supplementary Figure S1

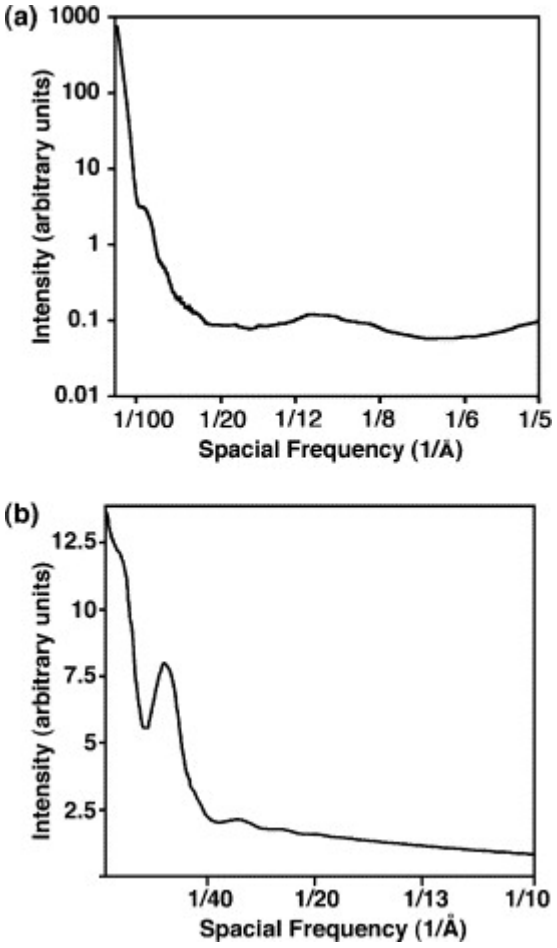


Supplementary Figure S2

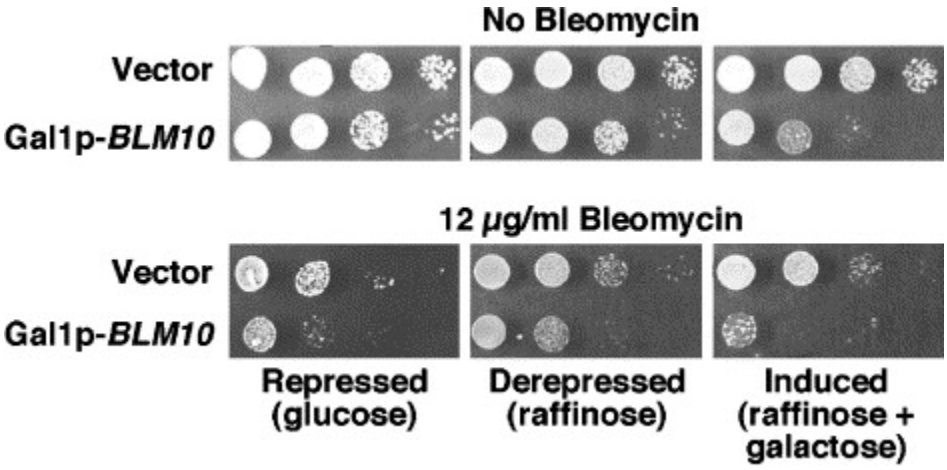


Supplementary Figure S3

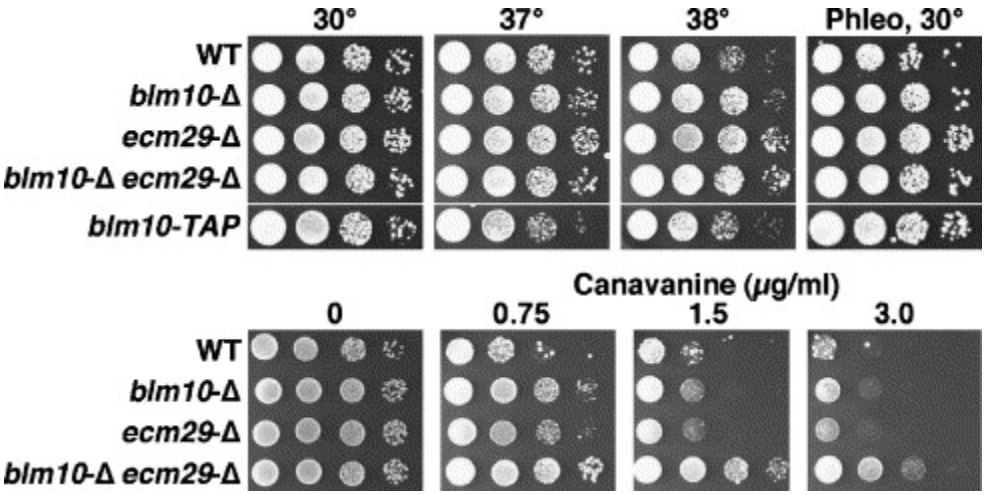


Supplementary Figure S4